Circulating and Eddy Current Losses in Coreless Axial Flux PM Machine Stators with PCB Windings

Yaser Chulaee, *Student Member, IEEE*, Donovin Lewis, *Student Member, IEEE*,
Ali Mohammadi, *Student Member, IEEE*, Greg Heins, *Member, IEEE*,
Dean Patterson, *Life Fellow, IEEE*, Dan M. Ionel, *Fellow, IEEE*

Abstract—Printed circuit board (PCB) stators in coreless axial flux permanent magnet (AFPM) machines have been proposed, designed, and studied for use in multiple industries due to their design flexibility and reduction of manufacturing costs, volume, and weight compared to conventional stators. This paper investigates mechanisms and methods of approximating open circuit losses in PCB stators within example wave and spiral winding topologies for a dual rotor, single stator configuration using 3D FEA, analytical hybrid techniques and experiments. The effect of rotor magnet shape, end winding, and active conductor geometry on eddy currents is studied, and some mitigation techniques are proposed. Through stator equivalent circuit analysis, circulating current losses caused by mechanical abnormalities and magnetic circuit asymmetry are assessed. Possible strategies and schemes to minimize circulating current losses are also described. The trade-off between stator loss components and some practical design considerations are outlined in detail. The open circuit power losses of a prototype coreless AFPM motor were experimentally tested using multiple example PCB stators and emulated rotor asymmetries, with the findings being comparable to the FEA and hybrid analytical methods results.

Index Terms—Axial-flux, coreless machines, FEA, permanent-magnet machines, PCB stator, winding losses, eddy current, circulating current.

I. INTRODUCTION

Interest in the development of axial flux permanent magnet synchronous machines (AFPMSMs) has grown in recent years with applications including electric vehicles (EVs), heating, ventilation, and air conditioning (HVAC) systems, and industrial motor drives, etc. Coreless machines have also grown in popularity, achieving ultra-high efficiency and high torque density by removing the magnetic core and associated losses. Combining both concepts to make coreless AFPM machines results in total AC losses dominated by those sourced from the stator windings.

The introduction of printed circuit board (PCB) stators in AFPM machines has become a trending topic due to their reduced weight and volume, ease of accurate manufacturability, and allowing for more accessible mass production [1]. The large flexibility in PCB stator coil shape, interconnection, and implementation has led to a multitude of studies focusing on their design and optimization for maximal efficiency [2]–[7]. Calculation of AC losses in PCB stators is essential towards winding design optimization prior to motor production as it contains the majority of component losses [5]. There are two major types of open circuit losses within stator winding: eddy current and circulating current losses. Eddy currents are due to varying flux density within a conductor, and circulating currents are caused by differences in induced voltages between conductors.

Previous work has proposed multiple methods and approaches for estimating the eddy current and circulating current losses in PCB stators. A closed form expression has been derived previously for the calculation of eddy current losses within PCB stator AFPM machines and shows how important the width of the active conductor is, especially for high-speed AFPMSM [5], [8], [9]. Eddy current losses in a PCB stator brushless motor have also been measured and approximated in prior work using a numerical method with a single magnetostatic solution and reasonable assumptions [10]. For the impact of rotor imbalance on circulating currents, the authors of [5] developed a relationship showing how the connection between layers directly contributes to power losses. Since each path is made up of a series of turns that are distributed across many layers, their corresponding back-EMF depends on where the individual traces are located.

Similarly in [6], it was proposed that rotor flux linkage between layer conductors are not the same, resulting in induced voltage differences between layers and circulating currents. As the number of layers increases, the difference in induced voltages increases, intensifying circulating currents [6]. Therefore, the selection of the number of layers, conductor paths, and their connected arrangement is essential. The analysis of mechanisms causing stator open circuit losses is important for the optimization of coil shape design, winding connections, and topologies.

In this paper, building upon previous studies describing wave [4], [5] and spiral [3], [11] winding topologies, two PCB stators with distinct topologies are designed, simulated, manufactured, and experimentally tested to investigate the mechanisms of open circuit losses, including eddy and circulating current losses. Three-dimensional FEA and analytical hybrid techniques for analyzing open circuit losses are discussed and some mitigation techniques have been presented [12]. Eddy current and circulating current simulations and experimentally measured results are reported for the example AFPM machines with PCB stators. Eddy current losses were studied both through direct numerical calculation and intuitive analysis of the potential eddy current path. The contributing factors towards circulating currents were studied through analytical methods and parametric simulations of mechanical and magnetic asymmetry. Experimental validation was performed to
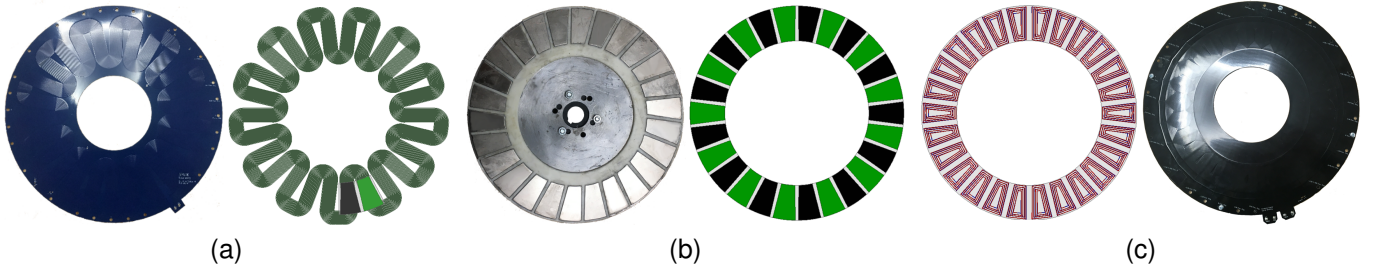
Fig. 1. Two different PCB stator simulation models and motor hardware components for the wave winding stator (a), dual 26 pole rotor (b), and the spiral winding stator (c) used for Ansys Maxwell simulation and the experimental motor prototype. Parameters of both stators are described in Table I.

study the impact of mechanical and magnetic asymmetries on open-circuit losses using a prototype test fixture with findings applicable to the evaluation of asymmetry resilience in future designs. This paper also provides a detailed discussion of the trade-off between stator power loss components, including eddy current losses, circulating current losses, and DC copper losses, and a systematic guideline for reducing these losses optimally in future designs while considering typical PCB manufacturing limitations and standards.

This paper is a follow-up expansion of a conference paper and further investigates the open circuit loss mechanisms of winding losses in coreless AFPM machines with PCB stators [13]. Section II introduces the manufacturing limitations of PCB stators, the two designs explored within this paper, and their specifications. Section III discusses the eddy current loss mechanism, methods of calculation, and potential solutions for reduction. Section IV introduces the circulating currents loss mechanism and major causes, its approximation using equivalent circuits and parametric studies, and proposes methods of mitigation. Rotor asymmetries are emulated to study circulating current losses with simulation and experimental results presented in Section V. The second-to-last section is devoted to a discussion of findings and uncovers the trade-off between stator loss components. A combination of the discussed mitigation techniques is presented, taking into account the PCB manufacturing constraints that could reduce eddy current and circulating current losses in future designs.

II. PRINTED CIRCUIT BOARD STATOR DESIGNS

Studied PCB stators are comprised of radial planar copper traces connected axially with copper plated holes, or vias, between layers. Due to the planar nature of these traces, connections layer to layer and radially along the PCB stator require detailed analysis to maximize radial trace alignment and torque output while maintaining effective slot fill factor (SFF), the ratio of copper to slot area.

One of the major limitations in PCB stators is current-carrying capability of the PCB traces for field generation and torque production. Connecting planes of conductors in parallel or increasing conductor cross-sectional area are two measures to address this issue with a trade-off between Joule losses, circulating current losses, and eddy current losses.

Stator eddy current losses are greatly reduced compared to conventional coreless AFPM machines due to the very

TABLE I
SPECIFICATIONS OF TWO DIFFERENT SINGLE PHASE PCB STATOR WINDINGS WITH A 0.2MM TRACE WIDTH.

Winding type	Layer connection	N_t	N_L	t_h [mm]	OD [mm]	ID [mm]	R_{ph} [Ohm]
Wave	Parallel	182	12	0.14	304.9	144.5	0.6
Spiral	Series	162	6	0.07	270.4	182.1	0.8

small conductor cross-sectional area [5]. Current capability, however, is decreased with conductor area reduction and leads to parallel connections between traces to mitigate Joule losses in single conductors. The introduction of parallel paths for multi-layer connections increases the likelihood of circulating current generation between traces with different induced voltages within PCB layers [6]. These factors have led to many alternative approaches and designs for winding coil shapes and interconnections in previous works and industry [14], all of which boast varying electromagnetic properties, greatly impacting machine performance.

The example wave-type PCB stator winding, shown in Fig. 1a, based on the topology explored in [11], [15] and optimized considering eddy losses in prior work [3], comprises 12 layers, 10 which contain active copper traces and two that are used as a path to route the return. On each active layer, there are 42 traces with a 0.14mm trace height, t_h, 0.2mm trace width, t_w, and 0.25mm isolation width, t_g, grouped in six planar parallel traces aggregated in series to form seven turns, a pattern which is repeated for all active layers. The equivalent number of turns per phase, N_t, is reported in Table I for the wave winding from the product of the number of turns in one layer, 7, and the number of poles, 26. Vias are used to connect layers in parallel to increase current-carrying capability. The wave winding configuration maximizes active radial length, can host many pole pairs, and allows for easy layer stacking, however the turns are constrained by the outer and inner radii and manufacturing precision [11].

The example spiral-type PCB stator winding, depicted in Fig. 1c and described previously in [4], [5], [16], comprises six layers, all of which are active, with a two-layer coil pattern that radially connects the input and output terminals. On each active layer, there are 26 coils, and each coil has 27 turns with an altered 0.07mm trace height. The other parameters, like phase resistance and physical dimensions, are
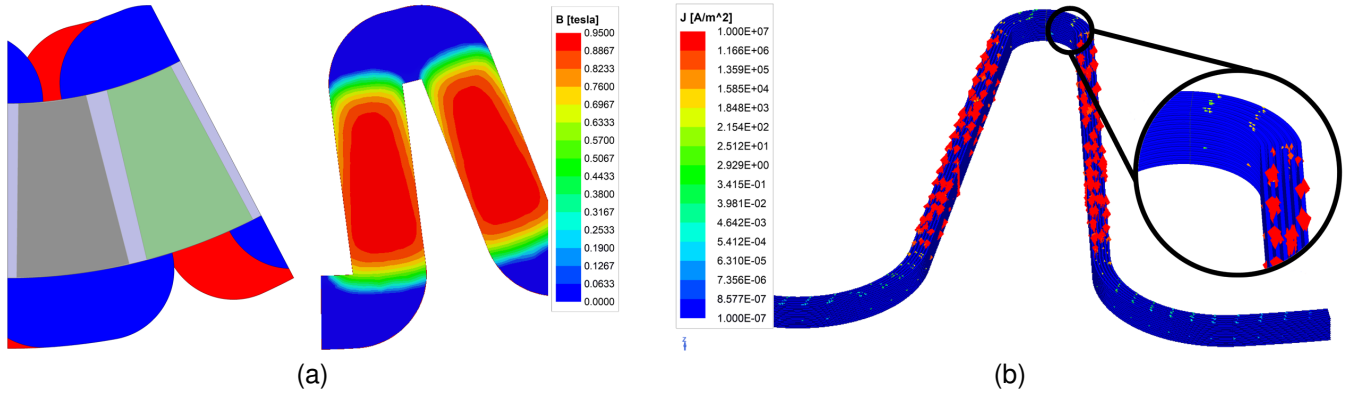
Fig. 2. Wave winding stator single pole pair 3D FE model and flux density distribution (a) and a diagram of the eddy current path in one turn (b). Since the dual rotor's magnets do not cover the coil's end windings, eddy current path is limited to the radial portion, shown in the detailed view.

summarized in Table I. Both configurations use a 26 pole rotor, shown in Fig. 1b on both sides to complete the flux path through the stator. Vias are used to connect all traces in series within one coil between layers and radially connect coils around the circumference via input/return bus bars. The spiral configuration maximizes coil area utilization, allows for a greater number of turns, and maximizes the torque to copper ratio, however it generates noncontributing torque due to angle relative to the motor center, and the active length is significantly shorter for inner tracks/turns [8].

The example PCB stator designs under study may not be suitable for direct comparison due to multiple differences in essential parameters. For example, in the wave winding stator a high number of layers were intentionally connected in parallel to study exaggerated circulating current losses between axially distributed stator conductors with no layer transposition. Another example is the thicker traces in the wave winding, close to the manufacturer's maximum capabilities, which are considered as a potential measure to improve current carrying capability and SFF without significant effect on eddy current losses, as it is discussed in Section VI.

III. Eddy Current Losses

One of the biggest challenges in coreless electric machine design is minimization of eddy current losses in stator windings. Without the protection of slots, windings in coreless AFPM machines are directly exposed to airgap flux density variations, causing eddy current within the stator's planar conductors [17], [18]. The power dissipation of these eddy currents is dependent on the conductor dimensions, material constants, and the operating frequency. The analytical methods for calculating eddy current losses originate from the following:

$$P_{ed} = \frac{1}{R} \left(\frac{d\varphi}{dt} \right)^2, \quad (1)$$

where R is the resistance and φ is the magnetic flux seen by the conductors. The relationship between PCB stator trace geometry and eddy currents losses can be approximated by the following [18]:

$$P_{ed} = \frac{\pi^2 N_c N_t f^2 t_w t_h l_m}{6\rho} \left(t_w^2 B_z^2 + t_h^2 B_\phi^2 \right), \quad (2)$$

where N_c is number of coil sides with average length of l_m; and N_t the turns per coil; B_z and B_ϕ are axial and tangential components of the flux density, respectively; t_w the trace width; t_h the trace height, in the z direction; and f denotes the frequency of flux variations. In accordance with this relationship, reducing the width of copper traces is necessary to minimize eddy current losses. However, this requires exploring methods to increase the current-carrying capacity to compensate.

Both PCB stators were designed with a focus on minimizing eddy currents by selecting a trace width significantly smaller than the skin depth at the machine's rated operating frequency. The skin depth of 2.5mm was calculated for the machine's rated frequency, f, of 650Hz using the equation $\delta = 1/\sqrt{\sigma f \mu_r \mu_0}$. A trace width of 0.2mm was chosen, which is an order of magnitude smaller than the skin depth, yet still manufacturable using state-of-the-art PCB fabrication technologies. In combination with layer transposition, as will be explained in the following sections, these narrow traces can replicate the effect of conventional Litz wire.

The example wave winding PCB stator, previously simulated and experimentally tested in [3], experiences eddy current losses caused by the shifting magnetic flux as indicated in Fig. 2a. The eddy current path, shown in Fig. 2b, is constrained to the radial conductor, preventing circulation through the system through the end winding as there is no flux nor current density.

The flux density mapping of the example spiral winding in Fig. 3a highlights that the rotor magnets fully cover the end winding during operation to utilize maximal active conductor but also extending a full eddy current path through the coil. Vias within the center of the coils are used for connections between layers and coil sections, allowing eddy current to move between layers within the region of varying flux density, as shown in Fig. 3b. Thereby eddy current can freely travel within the example spiral winding with great potential to
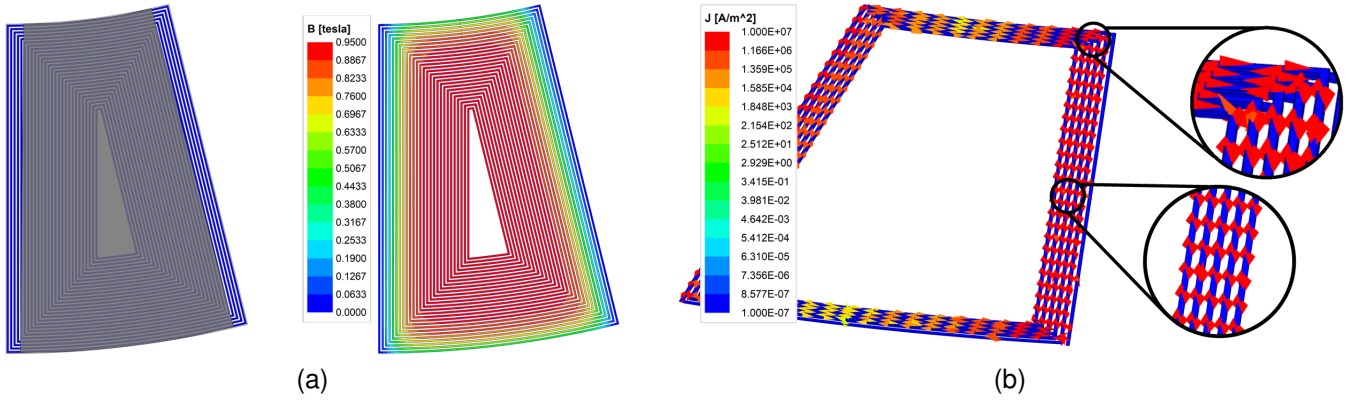
Fig. 3. Spiral winding stator single pole 3D FE model and flux density distribution (a) and a diagram of the eddy current path within 5 turns and 1 layers (b). Since the dual rotor's magnets cover the entire coil, eddy current path is not limited to the radial portion, propagating through the coil and from one layer to another.
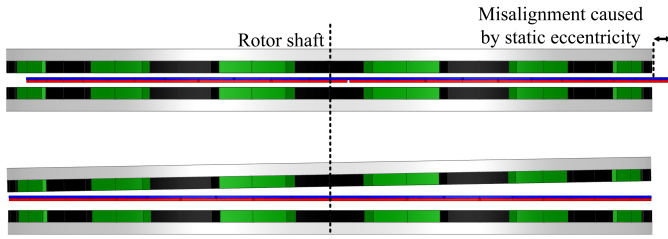

Fig. 4. Two rotor asymmetry conditions. Uneven airgap or tolerances in magnet remanences and static eccentricity.

propagate throughout the stator, increasing thermal losses throughout.

If a future design were to focus upon other objectives, limiting the eddy current path with coil geometry and magnet placement could significantly reduce the propagation of generated eddy currents and resulting losses. Since both PCB stator examples were designed to minimize eddy current, their measured and simulated loss contributions are minimal compared to the rated copper losses, as demonstrated in Tables III and IV.

IV. CIRCULATING CURRENT LOSSES

The parallelization of conductors is a typically considered method for reducing eddy currents while maintaining a high current-carrying capacity. Circulating currents are created through induced voltage differences in parallel conductors caused by a variety of factors ranging from conductor geometry and mechanical/magnetic asymmetry when exposed to airgap flux density variation. For instance, as the axial flux machine is highly susceptible to a mechanically varied airgap, imbalances in the amplitude of induced back-EMFs cause current to flow between parallel paths. The difference in the back-EMFs amplitude can also happen because of rotor magnets with different remanences.

When windings are connected in parallel, to reduce track width and maintain current-carrying capability, current in each winding layer may not be distributed equally due to leakage fluxes [1]. One set of authors stated that circulating currents

in a PCB stator result from differences in induced voltage between layers of conductors, increasing as more layers are used depending on the method of interconnection [6]. Another paper proposed reconfiguration of parallel winding turns to reduce circulating current and the utilization of back-emf to approximate these losses [19]. To better understand the impact of static rotor eccentricity on a PM motor's circulating current in its parallel-connected windings, the authors of [20] developed a novel theoretical expression. This paper discusses how neutral point connections in stator windings influence circulating currents caused by rotor eccentricity.

A general expression for the calculation of circulating current losses within n parallel paths can be described as follows with an equal resistance of R where the induced voltage of ith path is denoted by E_i:

$$P_{cr} = \sum_{i=1}^{n} RI_i^2 = \frac{1}{R} \sum_{i=1}^{n} \left[E_i - \frac{\sum_{i=1}^{n} E_i}{n} \right]^2. \qquad (3)$$

According to Eq. (3), it can be inferred that the circulating current losses are directly proportional to the square of the speed, as the back-EMFs vary in proportion to the speed.

Connection of conductors in parallel with varying distances from rotor magnets can significantly increase circulating current. The flux density lines across the magnetic airgap, which is typically large in outer rotor axial flux permanent magnet machines, are pictured in Fig. 6, which shows how planar parallel conductors are exposed to uneven flux density distribution due to the flux fringing effect. Different voltages are induced in axially distributed parallel conductors, leading to circulating current flow between layers. In this case, even with perfect rotor condition and the absence of manufacturing tolerances, there are circulating currents like those measured in the example wave stator.

The PCB stator may be offset with regard to the rotor due to installation imperfections, a condition known as static eccentricity (Fig. 4). The accumulation of tolerances in axial flux machines can result in eccentricity from non-parallel discs that provide an uneven airgap, stator and rotors that
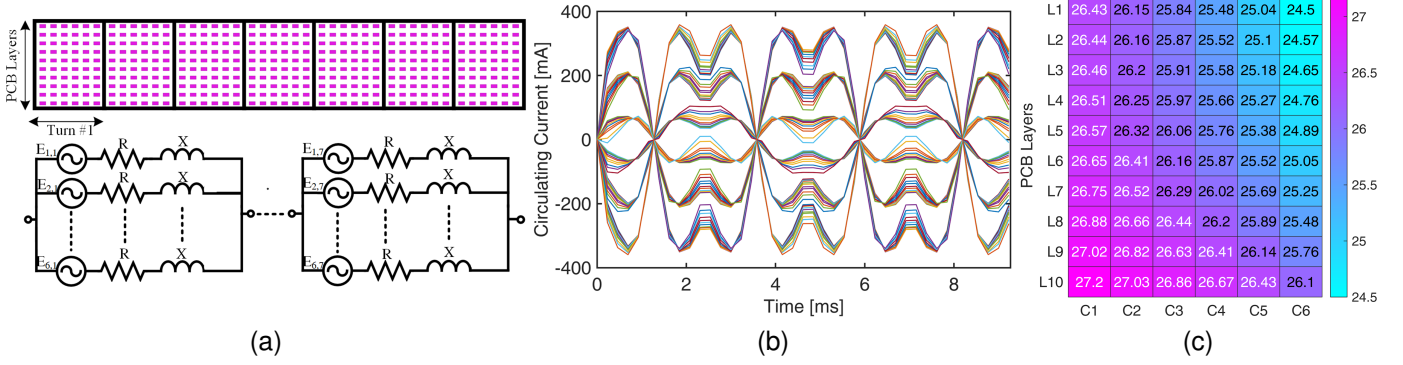
Fig. 5. Wave winding PCB stator diagrams including the conductor cross section for one phase and equivalent circuit for one layer (a), the open-circuit circulating currents in parallel traces within one turn (b), and a heat-map of the calculated induced voltages between copper traces within one turn over ten layers (c).
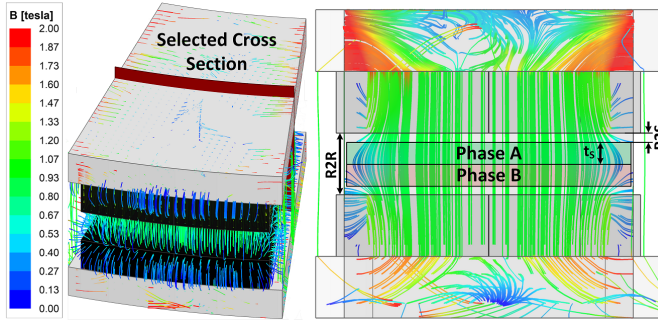
Fig. 6. Flux density lines across a cross section of the studied AFPMSM show fringing within the airgap. Differences in intensity of airgap flux density across parallel paths lead varying induced voltages and, consequently, circulating current losses.

Fig. 7. Transposing the coil geometry across layers as shown in (a) ensures a balanced induced back-emf between layers of planar conductor (b).

are not perfectly round, or any combination of these issues. Static eccentricity or imperfect magnet angular displacement can cause a phase shift in the back-EMFs of coils, resulting in distinct zero crossing points for induced voltages in coils as demonstrated with emulated eccentricity in Fig. 10. A circulating current will flow between coils experiencing different induced voltages as a result of system eccentricity and manufacturing tolerances. In conventional interior permanent magnet (IPM) machines, unequal currents in parallel paths caused by eccentricity leads to balancing magnetic forces [21]. Due to the extremely low winding inductance in coreless AFPM machines, these balancing forces are practically zero.

Circulating current losses can be significantly reduced by removing available parallel paths or balancing back EMFs between them. The removal of available parallel paths within the example spiral winding PCB significantly reduces circulating current, and would result in zero corresponding losses if there were perfect magnetic and mechanical symmetry. Transposition of coil connections between layers, like that shown in Fig. 7a is a well-known technique to mitigate circulating currents by balancing the back-EMFs in coil sections. Transposition geometrically balances the back-EMFs by ensuring all paths are impacted equally by airgap flux density variation, creating similar induced back-emf. Transposition, however, requires thorough investigation of the number of layers, poles, etc. for
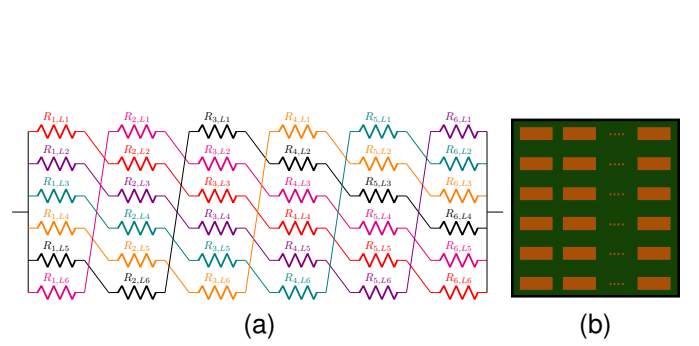
true implementation.

In order to adjust a motor design to the terminal voltage conditions, the number of equivalent turns in series per phases has to be selected. This must be done in coordination with the preferred dimensions of the PCB traces for manufacturing purpose and for minimization of losses, leading to the use of parallel paths. The asymmetries that exist in an electric machine, either due to abnormalities/faults, or due to the accumulated effect of material and manufacturing tolerances, may not be typically compensated in a current regulated permanent magnet synchronous machine by the use of parallel paths [21]. Nevertheless, these may cause though circulating losses, which can be particularly significant in coreless machines that have very low inductance and resistance, such as those considered in the studies.

To minimize the effect asymmetries, it is recommended to extend the parallel paths circumstantially for as many poles as possible and axially through as many PCB layers as possible. In the two prototypes studied in the current paper, this recommendation has been implemented, for historic development reasons, to a larger extent in the prototype with the wave winding. This is not to say that such a winding topology has an inherent advantage in terms of lower circulating current losses. In the studied wave and spiral winding example designs, parallel traces and coils were designed with typical
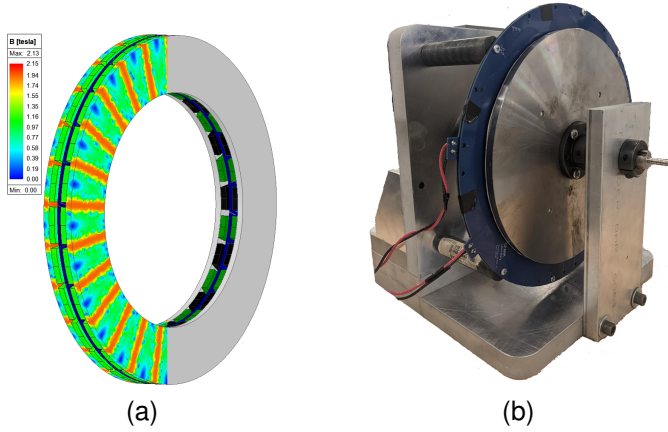
Fig. 8. The full 3D FEA model of the prototype machine employed for investigating the effect of rotor asymmetry on circulating current losses (a). The prototype single-stator, dual-rotor PCB stator coreless AFPM machine (b).

Fig. 9. The 3D FEA model for loss analysis that shows the employed tetrahedral mesh elements with zoomed-in views in different versions.

manufacturing dimensions to evaluate the effect of mechanical and magnetic abnormalities on circulating current losses. The authors conduct ongoing research, which will be covered in a future publication, to demonstrate a prototype design with spiral windings that employs the aforementioned recommendations for circumferential and axial parallel paths distribution resulting in virtually zero circulating current losses.

V. NUMERICAL AND EXPERIMENTAL STUDIES

Multiple 3D FEA models with millions of tetrahedral elements, one of which is presented in Fig. 8a, were designed in Ansys Maxwell [22] for loss analysis. For each model, a study was conducted to establish the minimum number of mesh elements required for accurate results by gradually reducing the number of elements until there were no significant changes in the results. Fig. 9 demonstrates the extremely high number of tetrahedral mesh elements present on PCB traces in the machine model (A) and the minimum required mesh elements utilized in all the studies (B). The computation time on an Intel Xeon 3.5-GHz workstation was approximately 15 hours.

Simulation results were experimentally validated with a prototype coreless AFPMSM shown in Fig. 8b. The main specification of the machine under study is also reported in Table II, considering one sample PCB per phase. Control of static eccentricity for uneven flux density distribution were built into the test fixture of the prototype to study the resulting circulating currents within both example stators.

Spin down tests were performed with rotor speed spun externally to a steady 1000rpm at which point the prime mover was decoupled and motor deceleration was measured with each PCB stator type. The experimental prototype's rotor inertia was calculated from the 3D model for each rotor to approximate it's contribution to deceleration. A plastic disc the same diameter as the PCB stator was used to separate mechanical and electromagnetic loss components similar to a process performed in [5], [23]. Open circuit loss components
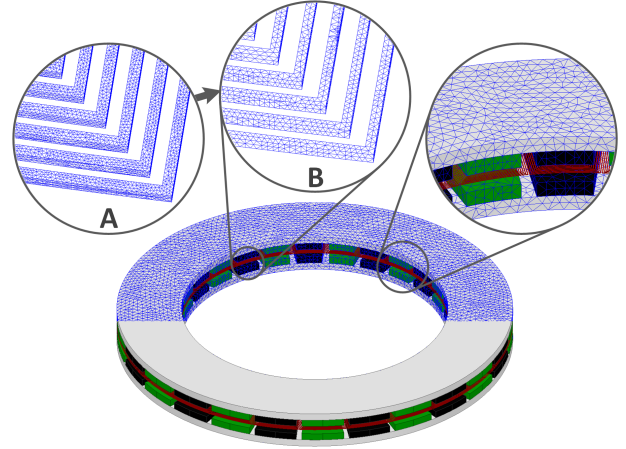
for both example PCB stators are numerically derived from FEA and analytical methods and verified by the measurements reported and discussed in the following sections.

A. Wave Winding Example

The measured and simulated single-phase back-EMFs of the example wave stator introduced in Section II are shown in Fig. 11 at 1000rpm which implies that there is a good agreement between the FEA-based and experimental results. The slight difference between measurements and FEA results may be attributed to typical material and manufacturing tolerances, including variations in magnet remanence, pole arc, etc.

The calculated eddy current loss within one phase at 1000rpm is 0.5W based on the trace by trace 3D FEA model shown in Fig. 2b and reported in Table III. The eddy current losses in this stator are a relatively small portion of stator copper losses at the aforementioned speed due to the selected narrow traces by the width of 0.2mm.

The circulating current power losses of the example wave design can be approximated analytically using Eq. (3) based on the stator equivalent circuit shown in Fig. 5a. Considering the 3D FEA results for rms circulating current in each trace, shown in Fig. 5b, and the resistance of each trace, as a function of length, resistivity, and cross-sectional area, the calculated total circulating current power loss in all 420 traces within one phase is 28.3W. The difference in induced voltages between conductors is depicted in Fig. 5c's heat map with the x-axis split into six planar parallel traces per turn and the y-axis representing ten active layers.

Even with perfect alignment and lack of manufacturing tolerances, circulating current losses in the wave winding would be significant due to the parallel paths distributed axially within the stator as non-uniform airgap flux density due to fringing effect induces different back-emfs throughout. The described method was validated experimentally using several spin-down tests and the results are illustrated in Fig. 12. The test was performed under identical conditions with a plastic
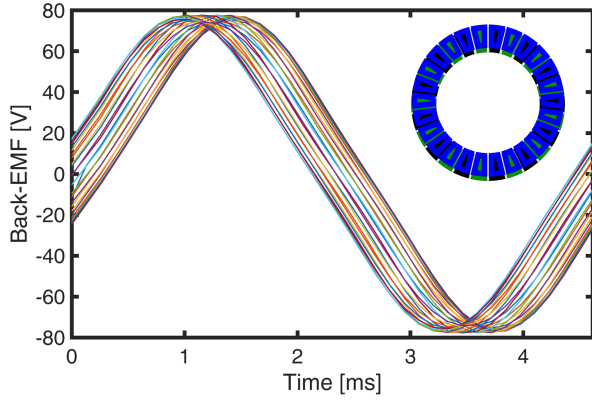
Fig. 10. Back-emf of the example spiral PCB stator's 26 coils with an exaggerated mechanical asymmetry or radial shift of 3mm. Variation in voltage amplitude creates circulating currents throughout the active stator portions.
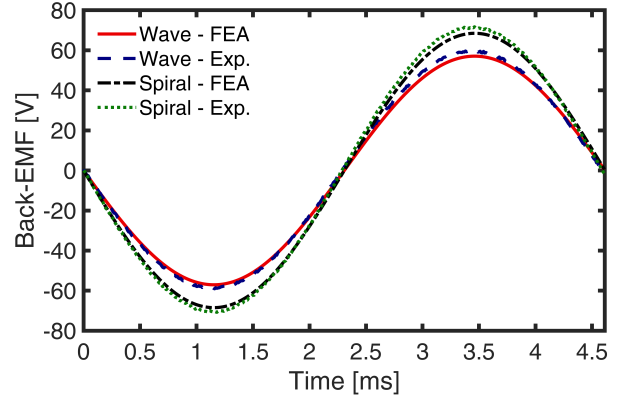

Fig. 11. Measured and simulated back-EMFs for both PCB stator examples across a full electrical period with the airgap of 1.5mm. Both the wave and spiral back-EMFs match between the experimental and simulated values.

TABLE II
SPECIFICATIONS AND MAIN DIMENSIONAL PROPERTIES OF THE STUDIED 26-POLE DOUBLE-ROTOR SINGLE-STATOR CORELESS PCB STATOR AFPM MACHINE.

Parameter	Value	Unit
Rated power	2.75	hp
Rated speed	3,000	rpm
Airgap (rotor to PCB)	1.5	mm
Rotor outer diameter	304	mm
Rotor inner diameter	208	mm
Rated copper losses	≈140	W
No. of rotor poles	26	-

TABLE III
PCB STATOR WITH WAVE TOPOLOGY; SINGLE PHASE COPPER LOSSES AT 1,000 RPM OPEN-CIRCUIT OPERATING CONDITIONS. SIMULATION RESULTS ARE BASED ON A COMBINATION OF FEA AND ANALYTICAL CALCULATIONS.

FEA and Analytical		Experimental
P_{cr} [W]	P_{ed} [W]	[W]
28.3	0.5	30.2

disc to separate mechanical and windage losses from the stator open circuit losses.

The resulting single-phase open circuit losses from the experimental, FEA, and analytical approximation methods at 1000rpm are summarized in Table III with the experimental losses closely matching the sum of circulating and eddy losses predicted. Results show that the majority of open circuit losses in the wave stator is circulating current losses, which can be as high as 15% of the total copper losses at rated torque. The wave topology is tolerant against rotor asymmetries as all traces in circumferential direction are connected in series.

Future development could adjust trace width and the number of parallel paths or implement layer transposition to greatly alleviate wave winding circulating currents originating from these parallel paths. By widening the trace width and reducing the number of parallel paths, the current carrying capacity can still be maintained while reducing the overall open circuit losses. Employing layer transposition as shown in Fig. 7a could make the wave topology a suitable candidate for PCB stator AFPM machines with greatly reduced circulating current losses.

B. Spiral Winding Example

The measured and FEA-based single-phase back-EMFs of the example spiral stator with the specification reported in Table I are depicted in Fig. 11 with similar results from both the experiment and the simulation. Eddy current losses in the example spiral type stator are low because the cross-section area of PCB traces is chosen to be much less than skin depth at the fundamental frequency. The single-phase eddy current losses within this example stator are 1.1W at 1000rpm as reported in Table IV. It should be highlighted that eddy current losses are proportional to the square of the rotor speed, according to (2).

Circulating currents within the spiral winding are greatly mitigated as the parallel paths within the active region are minimized, i.e., within one single coil there is no parallel connection. Rotor asymmetry leads to considerable amount of circulating current losses due to the sensitivity of stator conductors to flux density fluctuation in coreless AFPM machines resulting from the lack of protection of slots. New methods had to be developed to uncover the magnitude of circulating current losses as they are not related to the interconnection of coils radially or axially but to this asymmetry.

In order to investigate the effect of magnetic and mechanical asymmetries on circulating current losses, two parametric studies have been carried out, showing the trend of circulating current within the example design. In the first study, the remanence, B_r, of 4 magnets, one pole pair on each side, are gradually reduced in the simulation. This case, shown in Fig. 14, mimics the situation of uneven airgap and imperfection in magnetic material constants. The airgap flux density and consequently the back-EMFs of the coils under these bad magnets drop at any given time, causing circulating currents and associated losses.

Results of this study as reported in Fig. 15 show that a reduction of back-EMFs by 10% in two coils results in
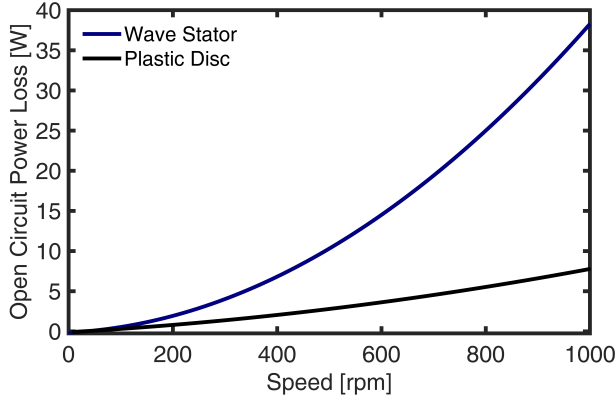
Fig. 12. Results of spin down experiments for the wave winding PCB stator to separate mechanical and magnetic losses using a dummy stator.
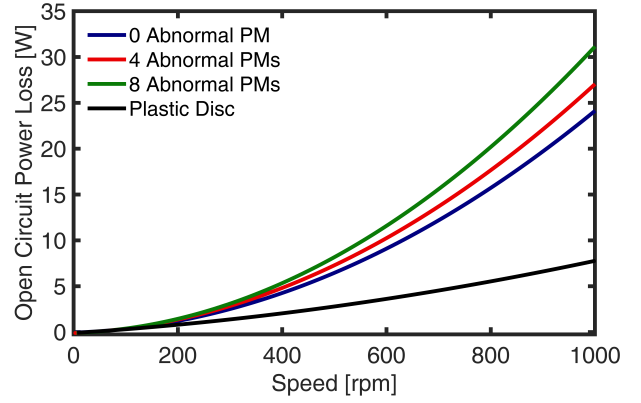

Fig. 13. Results of spin down experiments for the spiral winding PCB stator to investigate the impact of magnetic asymmetry on circulating current. Emulated asymmetry significantly increases expected power losses.

TABLE IV
PCB STATOR WITH SPIRAL TOPOLOGY; SINGLE PHASE COPPER LOSSES AT 1,000 RPM OPEN-CIRCUIT OPERATING CONDITIONS WITH INHERENT STATIC ECCENTRICITY. SIMULATION RESULTS ARE BASED ON A COMBINATION OF FEA AND ANALYTICAL CALCULATIONS.

Abnormal Pole Pairs	FEA and Analytical P_{cr} [W]	P_{ed} [W]	Experimental [W]
0	15.1	1.1	16.4
2	18.4	1.1	19.3
4	20.9	1.1	22.8

circulating current losses up to 6W. To experimentally validate the results of this parametric study at two specific points: 4 rotor magnets (1 pole pair), and 8 rotor magnets (2 pole pairs) were covered by steel sheets, emulating a rotor asymmetry situation. Steel sheets were also added to the rotor FEA model to simulate the effect on the airgap flux density and the back-EMFs of the coils. The experimental rotor and flux density distributions on the coils are demonstrated in Fig. 14. The flux density over the entire airgap drops by 20% under the covered magnets and results in approximately 7% reduction in the back-EMF of the coils.

The results of spin-down test scenarios with a normal rotor, one pole pair, and two pole pairs covered are demonstrated in Fig. 13. By covering one pole pair and two pole pairs on each rotor side, open circuit losses increases by 2.9W and 6.4W respectively within this stator. These results are fairly comparable with finite elements analysis results as reported in Table IV. Experimental results reported in Fig. 13 implies that even with no abnormal rotor magnet there is approximately 16W open circuit loss with a controlled static eccentricity within our text fixture subject to the second parametric study.

The second parametric study focused on the effect of static eccentricity on circulating current losses. In this mechanical asymmetry, the center of the PCB stator is shifted radially relative to the rotor as depicted in Fig. 4. The resulting back-EMFs of all coils with this exaggerated misalignment is

shown in Fig. 10. The simulation results presented in Fig. 15 indicate that a PCB stator offset by 0.75mm results in losses of approximately 15W. Correspondingly, the experimental results reported in the first row of Table IV show that the use of a normal rotor also leads to circulating current losses of 15.1W, equivalent to a controlled offset of 0.75mm in the PCB. From this study it can be concluded that the example stator has very large sensitivity to static eccentricity which is often caused by manufacturing/installation errors, bearing wear, etc.

Open circuit losses increased when the induced voltage angle difference between coils increased due to magnet displacement in the rotor or static eccentricity, and also as the voltage amplitude difference increased due to uneven airgap and variation in individual magnet remanence, both shown in Fig. 15 respectively. These studies indicate multiple potential sources of circulating current losses within parallel paths which should be simulated and accounted for in future development of similar machines. Circulating current losses within the spiral winding example would've been near zero without the discussed asymmetries due to the lack of parallel paths within a coil.

VI. DISCUSSIONS

A. Trade-off between Stator Winding Loss Components

The discussed open circuit losses in PCB stator windings are greatly affected by the geometry used for the planar conductors in each layer and the method of connections between them. The general tradeoffs between eddy current and circulating current losses in geometrical layout within a single phase PCB stator can be summarized as shown in Table V, assuming machine rated output torque and back-EMFs are maintained. As one independent variable, on the left of the table, is altered, other variables are changed to compensate for and maintain the current-carrying capability and output torque. The main parameters modified to trade between circulating and eddy current losses are the number of parallel paths, N_p; the number
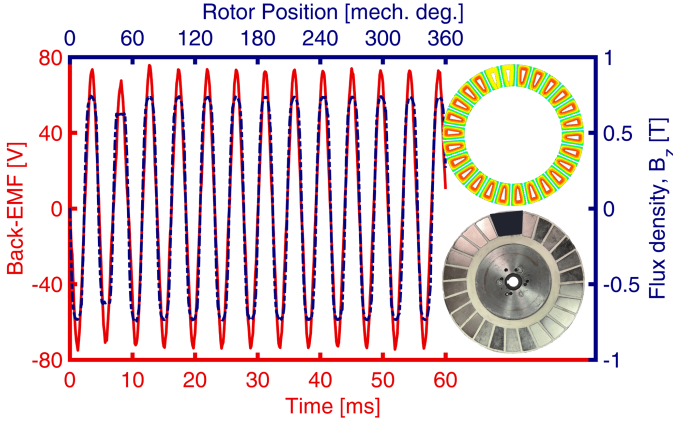
Fig. 14. Airgap flux density dips under the covered magnet pole pairs, which simulate magnetic asymmetry, reducing the resulting back-EMF in the spiral stator winding.
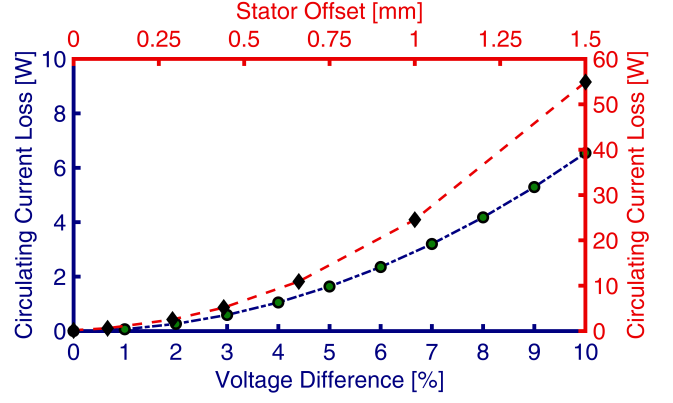

Fig. 15. Parametric study of circulating current losses derived from solving the equivalent circuit with variation in the emulated magnetic asymmetry in blue and mechanical asymmetry in red. A 10% difference in a pole-pairs back-EMFs relative to others causes around 6W of circulating current. Radial shifts in PCB stator relative to the rotors of 1mm results in approximately 25W of losses.

of turns, N_t; trace width, t_w; clearance between traces, t_l; and trace height, t_h, all within a single coil with a given coil width.

The expected changes in eddy current and circulating current power losses and the slot fill factor, which is inversely related to the Joule losses, are shown on the right side of the table as dependent variables. Analysis of the tradeoff between eddy current losses, circulating current losses, and Joule losses highlights opportunities to optimize PCB stator geometries and interconnections to minimize total copper losses and improve machine efficiency.

Eddy current losses are greatly impacted, by the trace width of planar conductors as shown in the analytical equation (2). The number of parallel paths also significantly impacts the circulating current losses. The SFF, or the ratio of copper to slot area within a coil side influenced by changes in trace width, height, and gap between traces and is correlated with machine power density and directly inverse to Joule losses. Increases to slot fill factor, through increased trace width or the number of parallel paths, result in increased eddy current losses and circulating current losses, respectively as shown in the first two rows of Table V.

In AFPM machines, the tangential component of flux density, B_ϕ, is an order of magnitude smaller than the axial component. Hence, based on (2), trace height, t_h, can be increased to maintain SFF while parallel path reduction without greatly increasing eddy current losses. Thicker traces in axial direction, increases total thickness of the PCB and leads to wider magnetic airgap and increased fringing effect. Currently, there are strict limitations for having conductor trace thickness by PCB manufacturers due to typical construction processes with minimum aspect ratios defined depending on the source.

Following these studies, a combination of the introduced mitigation techniques should be considered to minimize AC copper losses in the stator. Optimization of the coil envelope and magnet shape; minimization of the ratio of trace width to trace height; increasing the number of parallel paths to

improve Joule losses; considering true transposition to mitigate circulating current losses; and maximizing mechanical and magnetic symmetry have the largest impact on AC copper losses.

B. Increased Torque Production, Mechanical Airgap and PCB Thickness

The example spiral winding prototype employs two PCBs, one per phase, each with a thickness, t_{PCB}, of 1.2mm and has been assembled with a total gap between rotors, R2R, of 5.4mm, measured from magnet-to-magnet (see Fig. 6). This resulted in a relatively large mechanical per-side airgap, R2S, of 1.5m, measured from the face of the magnet to the PCB stator. The arrangement was selected in order to facilitate precise installation in the laboratory fixture under the very large magnetic forces between the two rotors, and to provide data for electromagnetic FEA model validation to further support a parametric design study, as explained in the following. The geometrical dimensions are related for a two-phase motor by the equation $t_{PCB} = (R2R - 2 \times R2S)/2$.

Maintaining R2R constant in the prototype and allowing R2S to be as low as 0.675mm provides space for substantially thicker PCBs of $t_{PCB} = 2mm$ to be used per phase. With such a larger PCB stator design, and for the same current density, the torque within the same overall physical envelope increases considerably, approximately in the ratio of the stator PCB thickness. Most of this increase, which is approx. 75% for the described example based on FEA, is due to the increased ratio of equivalent ampere-turns together with a small contribution of approx. 5% due to the fact that the stator current sheet and rotor magnets are physically closer to each other. Thicker PCB stators may be manufactured, in principle, using special technologies [24] and suitable cooling is required for the increased stator losses corresponding to the

TABLE V
TRADE OFF BETWEEN EDDY CURRENT AND CIRCULATING CURRENT LOSSES WHILE MAINTAINING OUTPUT TORQUE. DASHES AND BLUE DOUBLE-LINE ARROWS DENOTE NO CHANGE AND A DESIRABLE TREND, RESPECTIVELY.

Independent Variables				Dependent Variables		
N_p	t_w	t_g	t_h	SFF	P_{ed}	P_{cr}
-	↑	↓	-	⇑	↑	-
↑	-	-	-	⇑	-	↑
↓	↑	↓	-	-	↑	⇓
↓	-	-	↑	-	-	⇓
↑	↓	↑	↑	⇑	⇓	↑

larger torque within the same space.

VII. CONCLUSION

This paper investigated open circuit loss mechanisms for coreless AFPM synchronous machines integrating PCB stators with wave and spiral winding designs. For the studied windings, power loss components were individually approximated based on detailed 3D FE models, analytical methods, and experimental measurements. Spin down tests were used to experimentally assess open circuit losses within two example stators, and the results were found to be comparable to FE-based analytical methods.

The impact of conductor path on eddy currents within the stators was studied and potential reduction of eddy current losses in future PCB stator designs was explored through the optimization of the rotor magnets and coil shape to shorten the path. Circulating current loss estimation methods have been developed to approximate power losses in varying planar conductors. Furthermore, mechanical and magnetic asymmetry was found to contribute to losses and estimated using parametric equivalent circuit analysis and experimentation with emulated and controlled asymmetry. Techniques for simulating controlled misalignment are applicable for future PCB stator designs to minimize circulating current losses alongside eddy current reduction.

Parallel layers, used to improve current-carrying capability and Joule losses, can greatly increase circulating currents and associated losses. A complete layer transposition was introduced as an effective technique to significantly reduce circulating current losses between the parallel conductors. The trade-off between the stator loss components was systematically explained and can be considered as a guideline for future designs. Effective design recommendations are outlined to reduce losses considering PCB manufacturing standards and limitations.

ACKNOWLEDGMENT

REFERENCES

[1] Z. Ouyang and M. A. E. Andersen, "Overview of planar magnetic technology—fundamental properties," *IEEE Transactions on Power Electronics*, vol. 29, no. 9, pp. 4888–4900, 2014.

[2] O. Taqavi and S. M. Mirimani, "Design aspects, winding arrangements and applications of printed circuit board motors: a comprehensive review," *IET Electric Power Applications*, vol. 14, pp. 1505–1518, 2020.

[3] P. Han, D. Lawhorn, Y. Chulaee, D. Lewis, G. Heins, and D. M. Ionel, "Design optimization and experimental study of coreless axial-flux pm machines with wave winding pcb stators," in *2021 IEEE Energy Conversion Congress and Exposition (ECCE)*, 2021, pp. 4347–4352.

[4] D. Lawhorn, P. Han, D. Lewis, Y. Chulaee, and D. M. Ionel, "On the design of coreless permanent magnet machines for electric aircraft propulsion," in *2021 IEEE Transportation Electrification Conference Expo (ITEC)*, 2021, pp. 278–283.

[5] F. Marcolini, G. De Donato, F. G. Capponi, and F. Caricchi, "Design of a high speed printed circuit board coreless axial flux permanent magnet machine," in *2021 IEEE Energy Conversion Congress and Exposition (ECCE)*, 2021, pp. 4353–4360.

[6] N. S., S. P. Nikam, S. Singh, S. Pal, A. K. Wankhede, and B. G. Fernandes, "High-speed coreless axial-flux permanent-magnet motor with printed circuit board winding," *IEEE Transactions on Industry Applications*, vol. 55, no. 2, pp. 1954–1962, 2019.

[7] H. Changchuang, B. Kou, X. Zhao, X. Niu, and L. Zhang, "Multi-objective optimization design of a stator coreless multidisc axial flux permanent magnet motor," *Energies*, vol. 15, p. 4810, 06 2022.

[8] X. Wang, T. Li, P. Gao, and X. Zhao, "Design and loss analysis of axial flux permanent magnet synchronous motor with pcb distributed winding," in *2021 24th International Conference on Electrical Machines and Systems (ICEMS)*, 2021, pp. 1112–1117.

[9] G. Francois and B. Dehez, "Impact of slit configuration on eddy current and supply current losses in pcb winding of slotless pm machines," *IEEE Transactions on Industry Applications*, pp. 1–1, 2022.

[10] A. Ahfock and D. M. Gambetta, "Stator eddy-current losses in printed circuit brushless motors," *Iet Electric Power Applications*, vol. 5, pp. 159–167, 2011.

[11] F. Marignetti, G. Volpe, S. M. Mirimani, and C. Cecati, "Electromagnetic design and modeling of a two-phase axial-flux printed circuit board motor," *IEEE Transactions on Industrial Electronics*, vol. 65, no. 1, pp. 67–76, 2018.

[12] M. Rosu, P. Zhou, D. Lin, D. Ionel, M. Popescu, F. Blaabjerg, V. Rallabandi, and D. Staton, *"Multiphysics Simulation by Design for Electrical Machines, Power Electronics and Drives"*, J. Wiley - IEEE Press, 2017.

[13] Y. Chulaee, D. Lewis, G. Heins, D. Patterson, and D. M. Ionel, "Winding losses in coreless axial flux pm machines with wave and spiral pcb stator topologies," in *2022 IEEE Energy Conversion Congress and Exposition (ECCE)*, 2022, pp. 1–6.

[14] B. Anvari, P. Guedes-Pinto, and R. Lee, "Dual rotor axial flux permanent magnet motor using pcb stator," in *2021 IEEE International Electric Machines Drives Conference (IEMDC)*, 2021, pp. 1–7.

[15] S. Paul, M. Farshadnia, A. Pouramin, J. Fletcher, and J. Chang, "A comparative analysis of wave winding topologies and performance characteristics in ultra-thin printed circuit board axial-flux permanent magnet machine," *IET Electric Power Applications*, 03 2019.

[16] F. Tokgöz, G. Çakal, and O. Keysan, "Design and implementation of an optimized printed circuit board axial-flux permanent magnet machine," in *2020 International Conference on Electrical Machines (ICEM)*, vol. 1, 2020, pp. 111–116.

[17] R. Wang and A. Kamper, "Evaluation of eddy current losses in axial flux permanent magnet (afpm) machine with an ironless stator," in *Conference Record of the 2002 IEEE Industry Applications Conference. 37th IAS Annual Meeting (Cat. No.02CH37344)*, vol. 2, 2002, pp. 1289–1294 vol.2.

[18] N. Taran, D. M. Ionel, V. Rallabandi, G. Heins, and D. Patterson, "An overview of methods and a new three-dimensional fea and analytical hybrid technique for calculating ac winding losses in pm machines," *IEEE Transactions on Industry Applications*, vol. 57, no. 1, pp. 352–362, 2021.

[19] F. Copt, C. Koechli, and Y. Perriard, "Minimizing the circulating currents of a slotless bldc motor through winding reconfiguration," in *2015 IEEE Energy Conversion Congress and Exposition (ECCE)*, 2015, pp. 6497–6502.

[20] E. Maruyama, A. Nakahara, A. Takahashi, and K. Miyata, "Circulating current in parallel connected stator windings due to rotor eccentricity in permanent magnet motors," in *2013 IEEE Energy Conversion Congress and Exposition*, 2013, pp. 2850–2855.

[21] I. P. Brown, D. M. Ionel, and D. G. Dorrell, "Unbalanced operation of current regulated sine-wave interior permanent magnet machines," in *2010 IEEE Energy Conversion Congress and Exposition*, 2010, pp. 4123–4130.

[22] *Ansys® Electronics, version 21.2, 2021, ANSYS Inc.*

[23] G. Heins, D. Ionel, D. Patterson, S. Stretz, and M. Thiele, "Combined experimental and numerical method for loss separation in permanent magnet brushless machines," *IEEE Transactions on Industry Applications*, vol. 52, pp. 1–1, 01 2015.

[24] P. Guedes-Pinto, "An axial-flux motor for an electrified world: It combines the best of two motor designs to save weight and energy," *IEEE Spectrum*, vol. 59, no. 4, pp. 38–43, 2022.